Eur. J. Inorg. Chem. 2011, 2183–2334

D 3715

EurJIC

European Journal of Inorganic Chemistry

14/2011
2nd May Issue

IYC 2011
International Year of CHEMISTRY

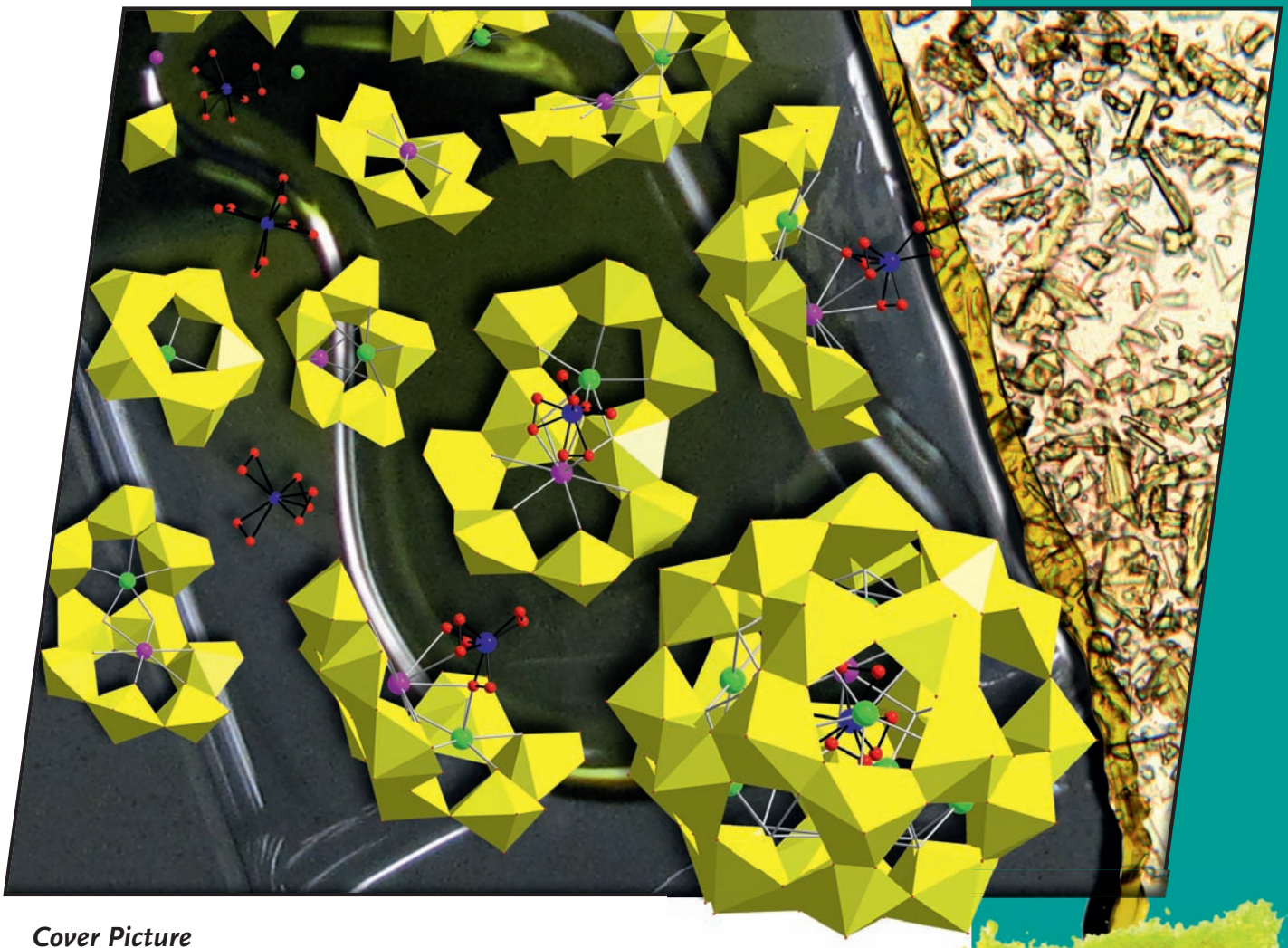

Cover Picture

May Nyman et al.

The U_{28} Nanosphere: What's Inside?

A Journal of

ChemPubSoc Europe

WILEY-VCH

www.eurjic.org

EJICFK (14) 2183–2334 (2011) · ISSN 1434-1948 · No. 14/2011

CONTENTS

FULL PAPERS

Uranium Cluster

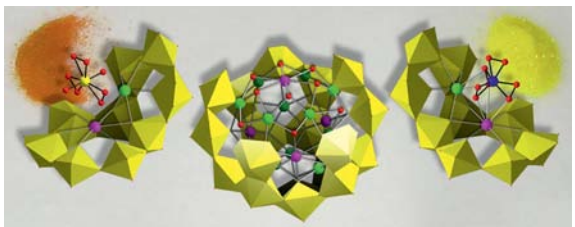

Reproducible, high-yield syntheses of uranyl peroxide polyoxometalates have been developed by strategic choice of internal templating cations and anions. We demonstrate irrefutably these clusters can be redissolved intact: a key point to fully developing the chemistry of actinide polyoxometalates.

Ba–Nb– Phosphate Compounds

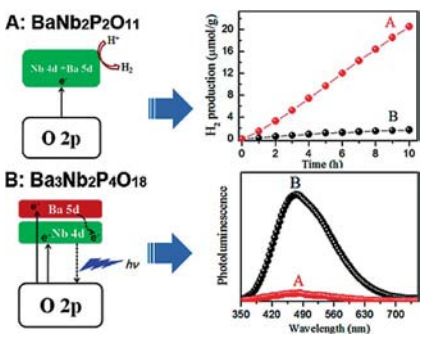

Two barium niobium phosphate compounds ($BaNb_2P_2O_{11}$ and $Ba_3Nb_2P_4O_{18}$) were prepared by a conventional solid-state reaction method. Although both compounds have similar optical band gaps (ca. 3.6 eV), their optical and photocatalytic behavior differs due to their different conduction band constructions, which results from their different crystal structure environments.

Yttrium-Vanadate Nanocrystals

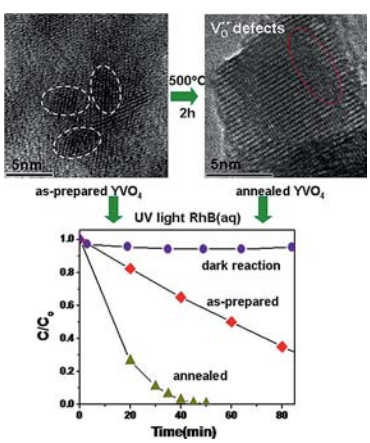

YVO_4 nanocrystals with controlled crystallinity and surface chemical states were successfully prepared. It is demonstrated that YVO_4 nanocrystals with high crystallinity and sufficient oxygen vacancies show optimum photocatalytic performance.

In-situ Synchrotron Diffraction

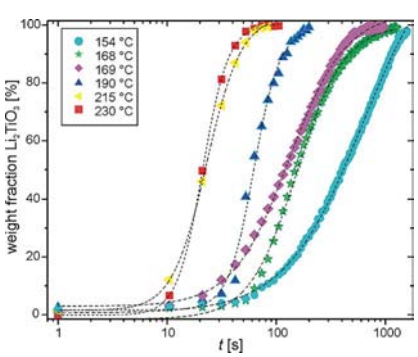

Hydrothermal syntheses, following the reaction $TiO_2(s) + 2\ LiOH(aq) \rightarrow Li_2TiO_3(s) + H_2O(l)$, are studied in-situ by synchrotron powder X-ray diffraction at varying temperatures. The formation of cubic Li_2TiO_3 shows increasing reaction rates at higher temperatures, which enables the determination of the activation energy.

Metal−Organic Frameworks

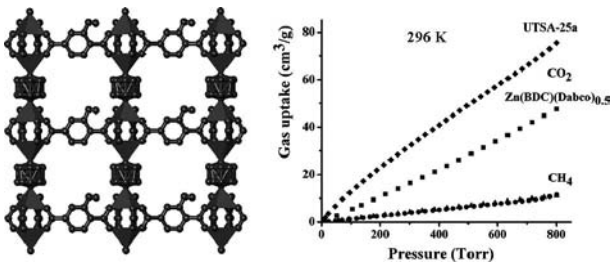

Keywords: Zinc / Microporous materials / Adsorption / Immobilization / Gas separation / Carbon dioxide

The 3D microporous metal−organic framework (MOF) $Zn(BDC\text{-}OH)(DABCO)_{0.5}$ (UTSA-25a; H_2BDC-OH = 2-hydroxybenzenedicarboxylic acid, DABCO = 1,4-diazabicyclo[2.2.2]octane) with functional −OH groups on the pore surfaces exhibits much higher selective CO_2/CH_4 separation than the original MOF $Zn(BDC)(DABCO)_{0.5}$ at ambient temperatures.

Hydrogen Generation

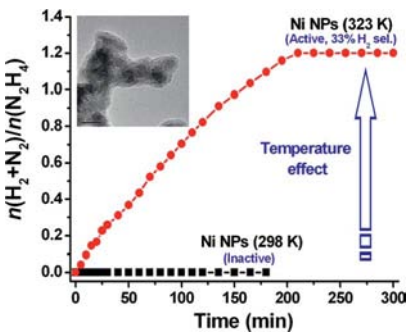

Keywords: Nickel / Hydrogen / Hydrazine / Nanostructures / Temperature effects

A drastic enhancement in the catalytic performance of Ni nanoparticles, which are inactive for the decomposition of hydrous hydrazine to hydrogen at room temperature, was observed with an increase of reaction temperature to 323 K. This temperature effect has been exploited to achieve 100% H_2 selectivity from hydrous hydrazine decomposition by alloying Ni and Pt with a Pt content as low as 1 mol-%.

^{18}F-Labelled Peptides

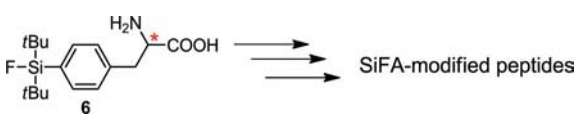

Keywords: Fluorine / Silicon / Radiopharmaceuticals / Synthesis design / Enantioselectivity / Amino acids

Both enantiomers of the SiFA-modified phenylalanine were synthesized and characterized. They are key compounds for the efficient synthesis of a large variety of SiFA-modified peptides, which, in turn, hold great potential for the development of novel ^{18}F-labelled radiopharmaceuticals.

Intercalations

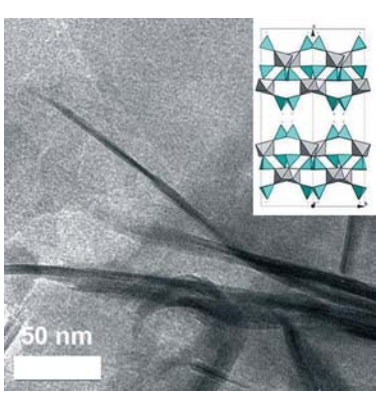

Keywords: Intercalations / Layered compounds / Adsorption / Organic−inorganic hybrid composites / Zeolite analogues

The synthesis of lamellar microporous titanosilicate AM-4 has been improved by varying the Ti source, autoclave time, and seeding. UZAR-S2 has been obtained by swelling and exfoliation of small crystals of AM-4.

CONTENTS

Photoreduction

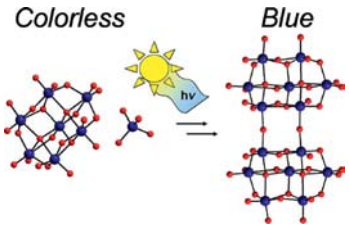

Colorless $(BuNH_3)_8[(Mo_7O_{24})(MoO_4)]\cdot 3H_2O$ ($BuNH_3$ = butan-1-aminium), which contains heptamolybdate and monomolybdate anions, is easily transformed to the blue dimer $(BuNH_3)_{10}[(Mo_7O_{22})(\mu_2\text{-}O)_2\text{-}(Mo_7O_{22})]\cdot 5.5H_2O$ under sun irradiation.

Selenium Hydrogen Bonding

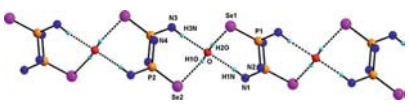

Bis(amido)-λ^3-cyclodiphosphazanes, *cis*-[R′(H)NP(μ-NR)]$_2$, were prepared and converted into their P^V derivatives of the type *cis*-[R′(H)N(E)P(μ-NR)]$_2$ [E = O, S, Se, N=P(O)(OPh)$_2$]. An intermolecular Se···H–O hydrogen bond between *trans*-[*t*Bu(H)N(Se)P(μ-NCy)]$_2$ and H_2O was observed.

Schiff Base Complexes

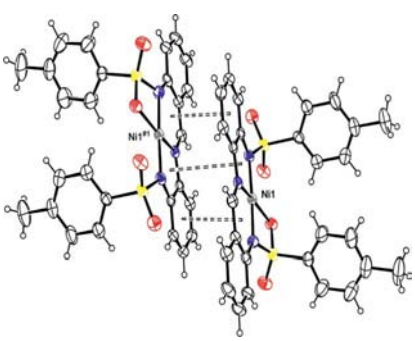

Homo- and heteroleptic metal(II) complexes (Co, Ni, Cu, Zn and Cd) containing the 2-(tosylamino)-*N*-[2-(tosylamino)benzylidene]aniline ligand have been synthesized by an electrochemical procedure and characterized by various spectroscopic techniques and single-crystal X-ray diffraction.

Organodiselone Ligands

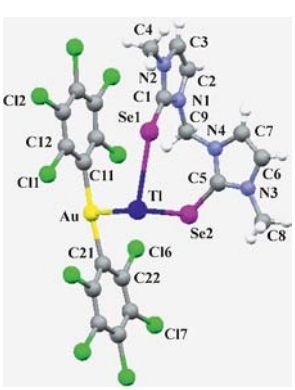

Homopolynuclear Tl^I and heteropolynuclear Au^I–Tl^I complexes that bear organodiselone ligands have been synthesized. The luminescence of the Au–Tl derivatives has been analyzed experimentally and theoretically through DFT calculations.

Thallium−Chalcogen Interactions

X-ray structural analysis of dimeric $[Me_2TlO(2,6\text{-}R_2C_6H_3)]_2$ (R = H, Me, *i*Pr, Ph) shows significant structural changes due to the increased steric bulk of the phenoxide ligand. Sufficient steric bulk is present when R = *t*Bu to facilitate isolation of a monomeric species. DFT calculations were employed to rationalize the observed structures.

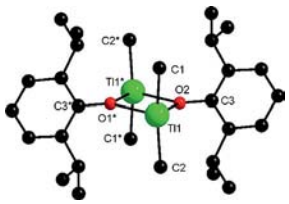

Keywords: Thallium / O ligands / Density functional calculations / Structure elucidation

Mixed-Valence Chemistry

Dimeric species of triruthenium cluster moieties exhibit six reversible one-electron redox processes and rich mixed-valence chemistry with strong cluster−cluster interactions across the asymmetric bis(tridentate) triazine ligand.

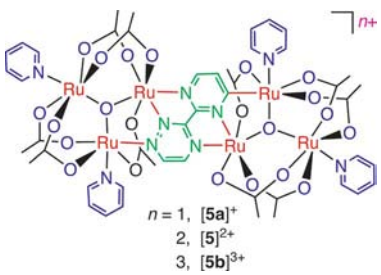

Keywords: Ruthenium / Cluster compounds / N ligands / Redox chemistry / Density functional calculations

Modifiable Magnetic Anisotropy

A series of valence-sandwich-type $Mn^{III}_4Mn^{II}_8$ clusters were synthesized by solvothermal reaction. Magnetization studies reveal that they all behave as single-molecule magnets (SMMs) and the ground-state anisotropy of four clusters are effectively modified by intra- and intermolecular interactions by substituting tripodal ligands and terminal ligands.

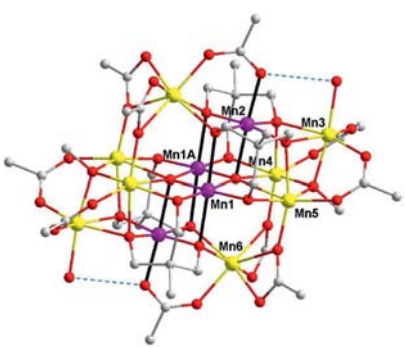

Keywords: Manganese / Tripodal ligands / Molecular interactions / Magnetic properties / Single-molecule magnets

Tunable Phosphors

New interesting luminescent $Gd_4Si_2O_7N_2$ materials doped with Ce^{3+}, Tb^{3+} or Dy^{3+} have been prepared and their luminescence properties have been studied. Under UV excitation, $Gd_4Si_2O_7N_2$:Ce^{3+} shows blue emission. The emission colour of $Gd_4Si_2O_7N_2$:Tb^{3+} and $Gd_4Si_2O_7N_2$:Dy^{3+} can be tuned.

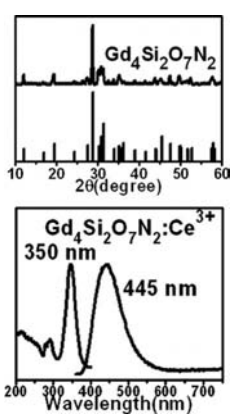

Keywords: Cerium / Terbium / Dysprosium / Luminescence

* Author to whom correspondence should be addressed.

Supporting information on the WWW (see article for access details).

This article is available online free of charge (Open Access).

If not otherwise indicated in the article, papers in issue 13 were published online on April 20, 2011

